Journal of Organometallic Chemistry, 368 (1989) 231–247
Elsevier Sequoia S.A., Lausanne – Printed in The Netherlands
JOM 09832

Synthesis and structure of five-coordinate bis(hydrocarbyl)iridium(III) complexes of the formula $Ir(R)R'[N(SiMe_2CH_2PPh_2)_2]$

Michael D. Fryzuk *, **Patricia A. MacNeil, Roberta L. Massey**
Department of Chemistry, University of British Columbia, 2036 Main Mall, Vancouver, B.C. V6T 1Y6 (Canada)

and Richard G. Ball *
Department of Chemistry, University of Alberta, Edmonton, Alberta T6G 2G2 (Canada)

(Received November 14th, 1988)

Abstract

Reaction of the hydrocarbyliridium(III)-halide complexes $Ir(R)X[N(SiMe_2CH_2PPh_2)_2]$ ($R = CH_3$, $X = I$; $R = CH_2Ph$, $X = Br$; $R = C_6H_5$, $X = I$) with organolithium reagents generates the coordinatively unsaturated, five-coordinate complexes $Ir(R)R'[N(SiMe_2CH_2PPh_2)_2]$, where R′ can be CH_3, CH_2CMe_3, CH_2SiMe_3, or C_6H_5. These highly colored, crystalline materials are trigonal bipyramidal in the solid state and in solution. The crystal structure of the dibenzyl derivative, $Ir(CH_2Ph)_2[N(SiMe_2CH_2PPh_2)_2]$, shows a distorted trigonal bipyramidal structure with the tridentate ligand occupying the two axial positions (PPh_2 donors) and one equatorial site (NSi_2); the two benzyl groups are at the remaining equatorial positions with the angle between these two ligands being 77.6 (1)°.

Introduction

Simple σ-bonded hydrocarbyl complexes of iridium have figured prominently in all facets of mechanistic and synthetic organometallic chemistry [1]. The fundamental processes of oxidative addition and reductive elimination, migratory insertion and deinsertion of CO, and β-elimination and olefin insertion [2], have all benefitted from model studies [1–3] using organoiridium complexes as either reactants or products. More recently, advances in carbon–hydrogen bond activation [4] have involved hydrocarbyliridium complexes at almost every stage.

By far, most of the alkyl and aryl complexes known for iridium are of Ir^{III} where the metal center is coordinatively saturated in an octahedral [5] or pseudo-octahedral ("piano-stool") environment [6]. One important example of the latter type

0022-328X/89/$03.50 © 1989 Elsevier Sequoia S.A.

is the complex (η^5-C_5Me_5)Ir(CO)H(CH_3) which is produced upon photochemical activation of methane by Ir(η^5-C_5Me_5)$(CO)_2$ [6e]. Square-planar Ir^I alkyls and aryls have been prepared [7]. These include the alkyl analogues to Vaska's compound which tend to be more reactive than IrCl(CO)$(PPh_3)_2$ due to the increased electron density at the metal center when a Cl is replaced by an alkyl group R [7h]. Remarkably, there are only a few examples of five-coordinate hydrocarbyl derivatives and those reported thus far contain just a single alkyl or aryl ligand [8].

As part of a general study, we have been developing the coordination chemistry of the tridentate, mixed-donor ligand $^-N(SiMe_2CH_2PR_2)_2$ with the transition metals [9] and the lanthanoids [10]. Target molecules are perhydrocarbyl complexes stabilized with the above ancillary ligand having a general formula $MR'_n[N(SiMe_2CH_2PR_2)_2]$. It is our intention to examine the effect of this ancillary ligand on the reactivity of coordinated hydrocarbyl groups as a function of the central metal M. In this paper, we present the full details for the preparation and characterization of complexes of the general formula $Ir(R)R'[N(SiMe_2CH_2PPh_2)_2]$ where R = CH_3, C_6H_5, CH_2Ph, and R' = CH_3, C_6H_5, CH_2Ph, CH_2CMe_3, or CH_2SiMe_3. These five-coordinate bis(hydrocarbyls) of Ir^{III} can be considered as formally 16-electron species and thus would be expected to show high reactivity.

Experimental

General information. All manipulations were performed under prepurified nitrogen in a Vacuum Atmospheres HE-553-2 glovebox equipped with a MO-40-2H purifier or in standard Schlenk-type glassware on a vacuum line. $IrCl_3 \cdot xH_2O$ was obtained from Johnson–Matthey and was used as received to prepare Ir(η^2-C_8H_{14})$[N(SiMe_2CH_2PPh_2)_2]$ and $Ir(CH_3)I[N(SiMe_2CH_2PPh_2)_2]$ as outlined in a previous publication [11].

Toluene, diethyl ether (Et_2O) and hexanes were purified by refluxing over dark blue or purple solutions of sodium-benzophenone ketyl ($NaPh_2CO$) followed by distillation under argon. Deuterated benzene (C_6D_6) was purchased from Aldrich, dried over activated 4Å molecular sieves, vacuum-transferred, and freeze-pump-thawed for several cycles prior to use.

Carbon, hydrogen, and nitrogen analyses of these air- and moisture-sensitive compounds were expertly performed by Mr. Peter Borda of this department. ^1H NMR spectra were recorded on either a Varian XL-300 spectrometer (300 MHz) or a Bruker WH-400 spectrometer (400 MHz). $^{13}C\{^1H\}$ and $^{31}P\{^1H\}$ NMR spectra were recorded on a Varian XL-300 spectrometer (75.43 MHz and 121.421 MHz, respectively). The $^{31}P\{^1H\}$ NMR spectra were referenced to external $P(OMe)_3$ set at +141.0 ppm relative to 85% H_3PO_4. NOEDIFF experiments were carried out on a Bruker WH-400 spectrometer (400 MHz) using standard pulse sequences.

All reagents were obtained in the highest purity possible. The organolithium reagents were prepared as described in the literature ($LiCH_2CMe_3$ [12], LiC_6H_5 [13], $LiCH_2SiMe_3$ [14], $LiCH_2C_6H_5 \cdot$TMEDA [15]) or used as received from Aldrich ($LiCH_3$, 1.4 *M* solution in Et_2O).

$Ir(CH_3)R'[N(SiMe_2CH_2PPh_2)_2]$, R' = CH_3, CH_2CMe_3, C_6H_5, CH_2SiMe_3

To $Ir(CH_3)I[N(SiMe_2CH_2PPh_2)_2]$ in toluene was added a toluene (or toluene/Et_2O for R' = C_6H_5 or Et_2O for R' = CH_3) solution of the appropriate organolithium reagent at 20 ° C, resulting in immediate colour changes from green to red or purple solutions. After stirring for 0.5 h, the solvent was removed in vacuo and the residue extracted with hexanes, filtered through Celite and reduced to dryness. Recrystallization from toluene/hexanes or neat hexanes at room temperature (or by cooling to -30 ° C), followed by decantation and vacuum drying gave products in isolated yields ranging from 60–80%.

$Ir(CH_3)_2[N(SiMe_2CH_2PPh_2)_2]$: $^{31}P\{^1H\}$ NMR (C_6D_6) 19.67 ppm (s). Anal. Found: C, 51.24; H, 5.80; N, 1.86. $C_{32}H_{42}IrP_2Si_2N$ calcd.: C, 51.18; H, 5.64; N, 1.86%.

$Ir(CH_3)CH_2CMe_3[N(SiMe_2CH_2PPh_2)_2]$: $^{31}P\{^1H\}$ NMR (C_6D_6) 11.53 ppm (s). Anal. Found: C, 53.71; H, 6.26; N, 1.59. $C_{36}H_{50}IrP_2Si_2N$ calcd.: C, 53.57; H, 6.24; N, 1.74%.

$Ir(CH_3)C_6H_5[N(SiMe_2CH_2PPh_2)_2]$: $^{31}P\{^1H\}$ NMR (C_6D_6) 16.56 ppm (s). Anal. Found: C, 55.54; H, 5.50; N, 1.60. $C_{37}H_{44}NIrP_2Si_2 \cdot \frac{1}{4}C_7H_8$ calcd.: C, 55.66; H, 5.54; N, 1.68%.

$Ir(CH_3)CH_2SiMe_3[N(SiMe_2CH_2PPh_2)_2]$: $^{31}P\{^1H\}$ NMR (C_6D_6) 13.51 ppm (s). Anal. Found C, 51.00; H, 6.00; N, 1.67. $C_{35}H_{50}IrP_2Si_3N$ calcd.: C, 51.07; H, 6.12; N, 1.70%.

$Ir(C_6H_5)I[N(SiMe_2CH_2PPh_2)_2]$

$Ir(CH_3)I[N(SiMe_2CH_2PPh_2)_2]$ was heated overnight at 80 ° C with stirring in benzene followed by solvent removal in vacuo and recrystallization from toluene/hexanes to give olive green crystals in 70% yield. $^{31}P\{^1H\}$ NMR (C_6D_6): 10.66 ppm(s); ^1H NMR (C_6D_6): $Si(CH_3)_2$, -0.11 (s), 0.52 (s); PCH_2Si, 1.57 (dt, J_{app} 5.4 Hz, J_{gem} 13.4 Hz), 1.77 (dt, J_{app} 5.6 Hz); $Ir\text{–}C_6H_5$, 6.29 (t, *meta*, J(H) 7.7 Hz), 6.54 (t, *para*, J(H) 7.1), 6.84 (d, *ortho*, J(H) 9 Hz); $P(C_6H_5)_2$, 7.01 (m, *meta/para*), 7.55 (m, *ortho*), 7.84 (m, *ortho*). Anal. Found: C, 47.80; H, 4.74; N, 1.36. $C_{36}H_{41}NIrP_2Si_2 \cdot \frac{1}{4}C_7H_8$ calcd.: C, 47.83; H, 4.57; N, 1.48%.

$Ir(C_6H_5)R'[N(SiMe_2CH_2PPh_2)_2]$, $R' = C_6H_5$, CH_2CMe_3

The syntheses of these complexes were carried out as described for the $Ir(CH_3)R'[N(SiMe_2CH_2PPh_2)_2]$ analogues above.

$Ir(C_6H_5)_2[N(SiMe_2CH_2PPh_2)_2]$: $^{31}P\{^1H\}$ NMR (C_6D_6) 11.22 ppm (s). Anal. Found C, 57.66; H, 5.40; N, 1.53. $C_{42}H_{46}IrP_2Si_2N$ calcd.: C, 57.64; H, 5.30; N, 1.60%.

$Ir(C_6H_5)CH_2CMe_3[N(SiMe_2CH_2PPh_2)_2]$: $^{31}P\{^1H\}$ NMR (C_6D_6): 11.77 ppm (s). Anal. Found: C, 58.18; H, 5.88; N, 1.55. $C_{41}H_{52}NIrP_2Si_2 \cdot \frac{1}{2}C_7H_8$ calcd.: C, 58.40; H, 6.17; N, 1.53%.

$Ir(CH_2C_6H_5)Br[N(SiMe_2CH_2PPh_2)_2]$

To a toluene solution of $Ir(\eta^2\text{-}C_8H_{14})[N(SiMe_2CH_2PPh_2)_2]$ was added 1.1 equivalents of $C_6H_5CH_2Br$ which was then stirred in the dark for 24 h. Solvent removal follwed by recrystallization from toluene/hexanes gave bright green crystals in 80% yield. $^{31}P\{^1H\}$ NMR (C_6D_6): 0.10 ppm (s). ^1H NMR (C_6D_6): $Si(CH_3)_2$, -0.23 (s), 0.46 (s); PCH_2Si, 1.55 (q of t, J_{gem} 15 Hz, J_{app} 5 Hz); $Ir\text{–}CH_2C_6H_5$, 4.95 (t, ^3J(P) 5.0 Hz); $Ir\text{–}CH_2C_6H_5$, 6.65 (t, *meta*, J(H) 8 Hz), 6.95 (t, *para*, J(H) 7.5 Hz), 7.28 (d, *ortho*, J(H) 8 Hz); $P(C_6H_5)_2$, 7.04 (m, *meta/para*), 7.91 (m, *ortho*). Anal. Found: C, 49.58; H, 5.00; N, 1.53. $C_{37}H_{43}BrIrNP_2Si_2$ calcd.: C, 49.82; H, 4.86; N, 1.57%.

$Ir(CH_2C_6H_5)R'[N(SiMe_2CH_2PPh_2)_2]$, $R' = CH_3$, $CH_2C_6H_5$, CH_2SiMe_3, C_6H_5

Method as for $Ir(CH_3)R'[N(SiMe_2CH_2PPh_2)_2]$ analogues described above [16]. $Ir(CH_2C_6H_5)CH_3[N(SiMe_2CH_2PPh_2)_2]$: $^{31}P\{^1H\}$ NMR (C_6D_6) 12.87 ppm (s). Anal. Found: C, 55.40; H, 5.50; N, 1.65. $C_{38}H_{46}IrNP_2Si_2$ calcd.: C, 55.18; H, 5.61; N, 1.69%.

$Ir(CH_2C_6H_5)_2[N(SiMe_2CH_2PPh_2)_2]$: $^{31}P\{^1H\}$ NMR (C_6D_6) 4.96 ppm (s). Anal. Found: C, 58.70; H, 5.50; N, 1.52. $C_{44}H_{50}IrNP_2Si_2$ calcd.: C, 58.51: H, 5.58; N, 1.55%.

$Ir(CH_2C_6H_5)CH_2SiMe_3[N(SiMe_2CH_2PPh_2)_2]$: $^{31}P\{^1H\}$ NMR (C_6D_6) 7.43 ppm (s). Anal. Found: C, 56.30; H, 6.26; N, 1.20. $C_{41}H_{54}IrNP_2Si_3$ calcd.: C, 56.54; H, 6.18; N, 1.48%.

$Ir(CH_2C_6H_5)C_6H_5[N(SiMe_2CH_2PPh_2)_2]$: $^{31}P\{^1H\}$NMR (C_6D_6) 11.68 ppm (s). Anal. Found: C, 58.87; H, 5.64; N, 1.57. $C_{45}H_{48}IrNP_2Si_2$ calcd.: C, 59.19; H. 5.30; N, 1.53%.

X-ray crystallographic analysis

Data collection. An irregular red-brown crystal of $Ir(CH_2C_6H_5)_2[N(SiMe_2CH_2PPh_2)_2]$, having approximate dimensions of 0.53 × 0.30 × 0.21 mm, was mounted in a 50/50 mixture of Paratone 717 and mineral oil, on a glass fiber in a non-specific orientation, on an Enraf Nonius CAD4 automated diffractometer. The crystal was cooled to −40 °C using a cold air-stream apparatus and all measurements were made at this temperature. The crystals are extremely air sensitive so the combination of oil coating and low temperature was used to protect the crystals from decomposition. All intensity measurements were performed using Mo-K_α-radiation (λ 0.71073 Å) with a graphite crystal, incident beam monochromator.

The automatic peak search and reflection indexing programs [17] in conjunction with a cell reduction program showed the crystal to be triclinic with possible space groups $P1$ and $P\bar{1}$.

The space group $P\bar{1}$ (No. 2) [18] was chosen and this choice confirmed by the successful refinement of the structure.

Cell constants were obtained from a least-squares refinement of the setting angles of 23 reflections in the range $15 < 2\theta < 24°$. The various crystal parameters are given in Table 1. The intensity data were collected using an ω–2θ scan ranging in speed from 10.1 to 2.0 deg/min (in ω). The variable scan rate was chosen to give $\sigma(I)/I \leq 0.30$ within 45 s in order to achieve improved counting statistics for both intense and weak reflections in a minimum time. The scan range was determined as a function of ω to compensate for the α_1–α_2 wavelength dispersion: (ω scan width (deg) $= 0.80 + 0.35 \tan \theta$). Backgrounds for the peaks were measured by extending the scan 25% on either side of the calculated range to give a peak to background counting time of 2/1. Intensity measurements were made out to a maximum 2θ of 55.0 °. There were 2 reflections which were chosen as standard reflections and these were remeasured every 120 min of exposure time to check on crystal and electronic stability over the course of data collection. These reflections changed in intensity by −1.3 and −1.9%, respectively, over the time span of data collection, which was considered negligible.

Data reduction. A total of 9826 reflections were collected and these were corrected for Lorentz, polarization and background effects according to the following formulae: $I = SR(SC - R^{*}B)/Lp$ and $\sigma(I) = \{SR(SC + R^2B) + (pI^2)\}/Lp^2$,

Table 1

Crystallographic data

Compound	$Ir(CH_2C_6H_5)_2[N(SiMe_2CH_2PPh_2)_2]$
Formula	$C_{44}H_{50}IrNP_2Si_2$
Crystal dimensions	0.53 × 0.30 × 0.21 mm
Triclinic space group	$P\,1$
a, Å	13.627(3)
b, Å	14.205(3)
c, Å	11.052(2)
α, deg	105.33(2)
β, deg	93.91(2)
γ, deg	91.41(2)
V, Å^3	2056.
Z	2
D_{calcd}, g/cm^3	1.459
μ, cm^{-1}	33.97
Radiation	Mo-K_α (λ 0.71073 Å)
Monochromator	Incident beam, graphite crystal
Take-off angle, deg	3.0
Detector aperture, mm	2.40 (horizontal) 4.0 (vertical)
Crystal-to-detector distance, mm	205
Scan type	$\omega-2\theta$
Scan rate, deg/min	10.1–2.0
Scan width in ω, deg	0.80 + 0.35 tan θ
Data collection 2θ limit, deg	55.0
Data collection index range	h, $\pm k$, $\pm l$
Reflections measured	9427 unique, 8038 with $I > 3\sigma(I)$
Observations/variables ratio	8038/451
Agreement factors R_1, R_2, GOF	0.027, 0.035, 1.24

where SR is the scan rate, SC is the total scan count, R is the ratio of scan time to background time, B is the total background count, p is a factor to down weight intense reflections (chosen as 0.040 in this experiment) and Lp is the Lorentz and polarization correction term.

After averaging equivalent forms (R-Factor for averaging is 0.025) and rejecting any systematically absent data there were 9427 unique reflections of which 8038, having $I > 3\sigma(I)$, were used in the structure solution and refinement.

Prior to assigning anisotropic thermal parameters an absorption correction was calculated using the absorption surface method of Walker and Stuart [19]. This correction applied coefficients ranging from 0.8899 to 1.2392 to F_0.

Structure solution and refinement [20]. The structure was solved using a three-dimensional Patterson synthesis which gave the positional parameters for the Ir atom. The remaining non-hydrogen atoms were located by the usual combination of least-squares refinement and difference Fourier synthesis.

Refinement of atomic parameters was carried out by using full-matrix least-squares techniques on F_o minimizing the function $\Sigma w(|F_o| - |F_c|)^2$, where $|F_o|$ and $|F_c|$ are the observed and calculated structure factor amplitudes respectively, and the weighting factor w is given by: $w = 4F_o^2/\sigma^2(F_o^2)$. The neutral atom scattering factors were calculated from the analytical expression for the scattering

Table 2

Bond lengths (Å) with estimated standard deviations in parentheses for $Ir(CH_2C_6H_5)_2[N(SiMe_2CH_2PPh_2)_2]$

Ir–P(1)	2.3148(8)	C(10)–C(11)	1.373(6)
Ir–P(2)	2.3125(8)	C(11)–C(12)	1.377(5)
Ir–N	2.113(3)	C(19)–C(20)	1.397(5)
Ir–C(31)	2.102(3)	C(19)–C(24)	1.390(5)
Ir–C(38)	2.125(3)	C(20)–C(21)	1.378(5)
P(1)–C(1)	1.843(3)	C(21)–C(22)	1.392(6)
P(1)–C(7)	1.827(3)	C(22)–C(23)	1.361(6)
P(1)–C(13)	1.818(3)	C(23)–C(24)	1.390(5)
P(2)–C(18)	1.822(4)	C(25)–C(26)	1.387(6)
P(2)–C(19)	1.824(3)	C(25)–C(30)	1.385(5)
P(2)–C(25)	1.834(3)	C(26)–C(27)	1.389(6)
Si(1)–N	1.715(3)	C(27)–C(28)	1.363(9)
Si(1)–C(13)	1.883(3)	C(28)–C(29)	1.377(8)
Si(1)–C(14)	1.883(4)	C(29)–C(30)	1.398(5)
Si(1)–C(15)	1.879(4)	C(31)–C(32)	1.496(4)
Si(2)–N	1.719(3)	C(32)–C(33)	1.382(5)
Si(2)–C(16)	1.872(4)	C(32)–C(37)	1.387(5)
Si(2)–C(17)	1.856(4)	C(33)–C(34)	1.387(5)
Si(2)–C(18)	1.888(4)	C(34)–C(35)	1.384(6)
C(1)–C(2)	1.385(4)	C(35)–C(36)	1.376(6)
C(1)–C(6)	1.389(5)	C(36)–C(37)	1.395(5)
C(2)–C(3)	1.385(5)	C(38)–C(39)	1.496(5)
C(3)–C(4)	1.381(6)	C(39)–C(40)	1.406(5)
C(4)–C(5)	1.383(6)	C(39)–C(44)	1.378(5)
C(5)–C(6)	1.396(5)	C(40)–C(41)	1.384(6)
C(7)–C(8)	1.387(5)	C(41)–C(42)	1.379(7)
C(7)–C(12)	1.395(5)	C(42)–C(43)	1.375(7)
C(8)–C(9)	1.391(5)	C(43)–C(44)	1.402(6)
C(9)–C(10)	1.377(6)		

factor curves [21]. The f' and f'' components of anomalous dispersion [22] were included in the calculations for all non-hydrogen atoms.

All hydrogens were included as fixed, isotropic atoms at their calculated positions, assuming C–H of 0.95 Å and appropriate sp^2 or sp^3 geometries. The methyl H's were fitted, by least-squares, to peaks observed in a difference Fourier. The thermal parameters assigned were 1.2 times those of the attached C atoms. During least-squares refinement the H atoms were constrained to 'ride' with the attached C atom.

In the final cycle 451 parameters were refined using 8038 observations having $I > 3\sigma(I)$. The final agreement factors were: $R_1 = \Sigma \| F_o | - | F_c \| / \Sigma | F_o | = 0.027$, and $R_2 = (\Sigma w(| F_o | - | F_c |)^2 / \Sigma w F_o^2)^{1/2} = 0.035$. The largest shift in any parameter was 0.008 times its estimated standard deviation and the error in an observation of unit weight was 1.24 e. An analysis of R_2 in terms of F_o, $\lambda^{-1}\sin\theta$, and various combinations of Miller indices showed no unusual trends. The highest peak in the final difference Fourier had an electron density of 1.0(1) e Å^{-3} and is without chemical significance. The bond distances and bond angles are listed in Tables 2 and 3 respectively. The atomic positional and thermal parameters, tables of anisotropic and equivalent isotropic thermal parameters, rms amplitudes of vibration,

Table 3

Bond angles (deg) with estimated standard deviations in parentheses for Ir$(CH_2C_6H_5)_2$[N$(SiMe_2CH_2$-$PPh_2)_2$]

P(1)–Ir–P(2)	170.25	C(7)–C(12)–C(11)	121.0(3)
P(1)–Ir–N	85.31(8)	C(21)–C(22)–C(23)	120.4(4)
P(1)–Ir–C(31)	94.08(9)	C(22)–C(23)–C(24)	120.5(4)
P(1)–Ir–C(38)	92.9(1)	C(19)–C(24)–C(23)	120.3(4)
P(2)–Ir–N	84.93(8)	P(2)–C(25)–C(26)	121.6(3)
P(2)–Ir–C(31)	93.60(9)	P(2)–C(25)–C(30)	119.4(3)
P(2)–Ir–C(38)	94.6(1)	C(26)–C(25)–C(30)	119.0(4)
N–Ir–C(31)	141.6(1)	C(25)–C(26)–C(27)	119.8(5)
N–Ir–C(38)	140.8(1)	C(26)–C(27)–C(28)	121.2(5)
C(31)–Ir–C(38)	77.6(1)	C(27)–C(28)–C(29)	119.8(4)
Ir–P(1)–C(1)	118.6(1)	C(28)–C(29)–C(30)	119.7(5)
Ir–P(1)–C(7)	119.4(1)	C(25)–C(30)–C(29)	120.4(4)
Ir–P(1)–C(13)	106.8(1)	Ir–C(31)–C(32)	111.1(2)
C(1)–P(1)–C(7)	103.0(1)	C(31)–C(32)–C(33)	121.1(3)
C(1)–P(1)–C(13)	100.0(1)	C(31)–C(32)–C(37)	121.1(3)
C(7)–P(1)–C(13)	107.0(2)	C(33)–C(32)–C(37)	117.8(3)
Ir–P(2)–C(18)	106.3(1)	C(32)–C(33)–C(34)	121.3(3)
Ir–P(2)–C(19)	116.0(1)	C(33)–C(34)–C(35)	120.3(4)
Ir–P(2)–C(25)	122.3(1)	C(34)–C(35)–C(36)	119.1(4)
C(18)–P(2)–C(19)	102.1(2)	C(35)–C(36)–C(37)	120.1(4)
C(18)–P(2)–C(25)	105.8(2)	C(32)–C(37)–C(36)	121.2(3)
C(19)–P(2)–C(25)	102.2(2)	Ir–C(38)–C(39)	111.7(2)
N–Si(1)–C(13)	107.3(1)	C(38)–C(39)–C(40)	120.8(3)
N–Si(2)–C(18)	106.5(1)	C(38)–C(39)–C(44)	121.7(3)
C(16)–Si(2)–C(17)	107.9(2)	N–Si(1)–C(14)	113.3(2)
C(16)–Si(2)–C(18)	107.0(2)	N–Si(1)–C(15)	112.4(2)
C(17)–Si(2)–C(18)	108.5(2)	C(13)–Si(1)–C(14)	110.2(2)
Ir–N–Si(1)	117.7(1)	C(13)–Si(1)–C(15)	105.2(2)
Ir–N–Si(2)	118.9(1)	C(14)–Si(1)–C(15)	108.1(2)
Si(1)–N–Si(2)	123.4(2)	N–Si(2)–C(16)	112.5(2)
P(1)–C(1)–C(2)	118.0(2)	N–Si(2)–C(17)	114.2(2)
P(1)–C(1)–C(6)	122.3(2)	P(1)–C(13)–Si(1)	109.4(2)
C(2)–C(1)–C(6)	119.3(3)	P(2)–C(18)–Si(2)	109.0(2)
C(1)–C(2)–C(3)	120.4(3)	P(2)–C(19)–C(20)	118.1(3)
C(2)–C(3)–C(4)	120.7(3)	P(2)–C(19)–C(24)	123.4(3)
C(3)–C(4)–C(5)	119.2(3)	C(20)–C(19)–C(24)	118.5(3)
C(4)–C(5)–C(6)	120.6(3)	C(19)–C(20)–C(21)	120.9(4)
C(1)–C(6)–C(5)	119.9(3)	C(20)–C(21)–C(22)	119.5(4)
P(1)–C(7)–C(8)	122.3(3)	C(40)–C(39)–C(44)	117.4(3)
P(1)–C(7)–C(12)	119.3(3)	C(39)–C(40)–C(41)	121.0(4)
C(8)–C(7)–C(12)	118.3(3)	C(40)–C(41)–C(42)	120.5(4)
C(7)–C(8)–C(9)	120.2(3)	C(41)–C(42)–C(43)	119.7(4)
C(8)–C(9)–C(10)	120.6(3)	C(42)–C(43)–C(44)	119.7(4)
C(9)–C(10)–C(11)	119.4(3)	C(39)–C(44)–C(43)	121.8(4)
C(10)–C(11)–C(12)	120.5(4)		

hydrogen atom parameters, torsion angles, and observed and calculated structure factors are available from Dr. R.G. Ball at the Structure Determination Laboratory, Department of Chemistry, University of Alberta. Inquiries regarding the crystallographic results should be directed to the above address quoting report number SR : 180702-01-86.

Results and discussion

Synthesis

Preliminary communications from our laboratory have reported [23,24] the preparation of methylhydrocarbyliridium(III) complexes $Ir(CH_3)R[N(SiMe_2CH_2PPh_2)_2]$ by reaction of RLi with the green, square-pyramidal methyl iodide complex $Ir(CH_3)I[N(SiMe_2CH_2PPh_2)_2]$ (**1a**). To extend this class of bis(hydrocarbyl) derivatives, we have developed routes to other five-coordinate, hydrocarbyl-halide derivatives. The bright green, benzyl bromide complex $Ir(CH_2Ph)Br[N(SiMe_2CH_2PPh_2)_2]$ (**1b**) is produced in 80% isolated yield by the oxidative addition of $PhCH_2Br$ to $Ir(\eta^2\text{-}C_8H_{14})[N(SiMe_2CH_2PPh_2)_2]$ in complete analogy to the preparation of **1a**. The phenyl-iodide complex $Ir(Ph)I[N(SiMe_2CH_2PPh_2)_2]$ (**1c**), cannot be accessed by oxidative addition, but rather heating the methyl-iodide derivative **1a** in pure benzene results in the elimination of methane [25] and the formation of the olive green complex **1c**. The structures of the new hydrocarbyl-halides **1b** and **1c** are completely analogous to that previously described [11]: the geometries are square-pyramidal with the hydrocarbyl group occupying the apical position.

The bis(hydrocarbyl) complexes are generated straightforwardly by addition of one equivalent of the appropriate organolithium derivative to the corresponding hydrocarbyl halide **1** (eq. 1). The reactions can be conveniently followed by the dramatic color changes from green to deep-red or purple. By NMR spectroscopy, these reactions are quantitative; isolated yields are generally 60–80% because of the high solubility of these complexes, however. These crystalline materials can be stored for several months under an inert atmosphere. In solution, they are extremely air- and moisture-sensitive, but remarkably thermally stable; for example, heating to 80 °C for extended periods (12–18 h) generally results in no change in the spectral properties for most of these complexes.

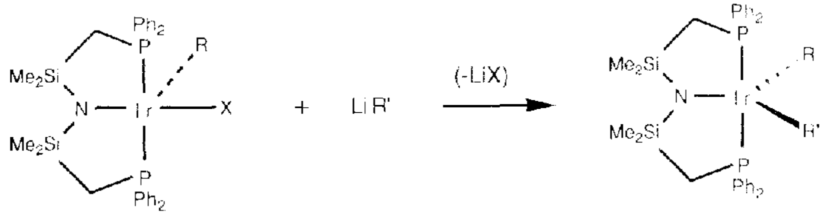

(1)

	R	X
1a	CH_3	I
1b	CH_2Ph	Br
1c	C_6H_5	I

	R	R'
2	CH_3	CH_3
3	CH_3	CH_2CMe_3
4	CH_3	C_6H_5
5	CH_3	CH_2SiMe_3
6	C_6H_5	C_6H_5
7	C_6H_5	CH_2CMe_3
8	CH_2Ph	CH_3
9	CH_2Ph	CH_2Ph
10	CH_2Ph	CH_2SiMe_3
11	CH_2Ph	C_6H_5

^{1}H and $^{13}C\{^{1}H\}$ NMR data

The proton NMR spectra of the bis(hydrocarbyl) complexes provide a valuable and straightforward method for their characterization. As for the resonances of the ligand backbone, there are two possible patterns that are observed depending on the hydrocarbon substituents at iridium. For those complexes where R = R′, and thus have C_{2v} symmetry, one observes very simple spectra consisting of a sharp singlet for the silyl methyl protons, a virtual triplet for the methylenes (due to coupling to the trans disposed phosphine donors), and one set of resonances for the ortho protons of the diphenylphosphino groups. This can be seen in Table 4 for the dimethyl (**2**), diphenyl (**6**) and dibenzyl (**9**) complexes in which there are equivalent environments above and below the metal tridentate plane. As for the rest of the complexes having only C_s symmetry, two singlets are observed for the silyl methyl protons as well as an AB quartet of virtual triplets for the methylenes and two sets of *ortho*-phenyl resonances.

The α-protons of the alkyl substituents on iridium have chemical shifts in the range of 0.51 ppm to 3.42 ppm, with the methyl and trimethylsilylmethyl α-protons being further upfield than those of the neopentyl and benzyl groups as would be expected. All show coupling to the phosphine ligands with $^{3}J(PH)$ ranging between 5.4 and 8 Hz.

As can be seen in the $^{13}C\{^{1}H\}$ NMR listed in Table 5, the methyl carbon bonded to iridium resonates anywhere between −31.60 and −22.06 ppm depending on the second hydrocarbon substituent. The methylene carbon of the trimethylsilylmethyl ligand is also found upfield between −24.22 and −14.37 ppm. As for those of the benzyl and neopentyl groups, the resonances are found further downfield between −4.22 to 4.13 ppm and 16.34 to 20.45 ppm, respectively. Although $^{13}C\{^{1}H\}$ NMR data for iridium alkyls are somewhat limited in the literature, there does seem to be some precedence for high field shifts for methyl carbons. For example, in the complexes $(\eta^{5}\text{-}C_5Me_5)Ir(PMe_3)(CH_3)X$ (X = Cl, CH_3, H) the methyl carbon resonance appears between −18.09 ppm and −37.96 ppm depending on the value of X [6j]. In the bis(hydrocarbyl) derivatives, **2**–**11**, two bond coupling to phosphorus ($^{2}J(PC)$) with values between 3.1 and 7.0 Hz can be observed for most of the carbon atoms bonded directly to iridium.

Solution structure

As described in a previous communication [24] for the methyl alkyl complexes $Ir(CH_3)R'[N(SiMe_2CH_2PPh_2)_2]$ (R′ = CH_3, CH_2CMe_3, CH_2SiMe_3, CH_2Ph), the five-coordinate iridium bis(hydrocarbyl) complexes have a trigonal bipyramidal geometry in both the solution and solid states on the basis of ^{1}H NMR, nuclear Overhauser effect difference (NOEDIFF [26]) experiments and X-ray diffraction studies. In particular, the NOEDIFF results clearly support this stereochemistry especially when contrasted to those results obtained for the square-pyramidal methyl halide complexes. In the latter situation, irradiation of the methylene protons of the ligand backbone gives rise to a positive NOE for the iridium methyl ($Ir\text{–}CH_3$) resonance of the complex $Ir(CH_3)Br[N(SiMe_2CH_2PPh_2)_2]$, indicating that the methyl is apical and *cis* to the amide donor. The analogous NOEDIFF experiment for the methyl iodide complex, **1a**, was complicated by a more complex multiplet for the methylene (PCH_2Si) resonance close in chemical shift to the iridium methyl ($Ir\text{–}CH_3$) resonance, thus obscuring any observable NOE. The

Table 4

^{1}H NMR spectral data ^{a} for the complexes Ir(R)R′[N(SiMe$_2$CH$_2$PPh$_2$)$_2$]

Ir(R)R′[N(SiMe$_2$CH$_2$PPh$_2$)$_2$]	Si(CH_3)$_2$	PCH_2Si	P(C$_6$$H_5$)$_2$	Other
2: R = R′ = CH$_3$	0.15 (s)	1.86 (t, J_{app} 5.0)	7.06 (m, *meta* / *para*)	Ir–CH_3, 0.94 (t, J(P) 6.0)
			7.61 (m, *ortho*)	
3: R = CH$_3$; R′ = CH$_2$CMe$_3$	0.12 (s)	1.80 (dt, J_{app} 5.0, J_{gem} 13.2)	7.11 (m, *meta* / *para*)	Ir–CH_3, 1.24 (t, J(P) 5.4)
	0.54 (s)	1.99 (dt, J_{app} 5.0)	7.61 (m, *ortho*)	Ir–CH_2C(CH$_3$)$_3$, 1.65 (t, J(P) 7.8)
			7.82 (m, *ortho*)	Ir–CH$_2$C(CH_3)$_3$, 0.82 (s)
4: R = CH$_3$; R′ = C$_6$H$_5$	0.17 (s)	1.83 (t, J_{app} 5.0)	7.06 (m, *meta* / *para*)	Ir–CH_3, 1.48 (t, J(P) 6.0)
	0.35 (s)		7.39 (m, *ortho*)	Ir–C$_6$$H_5$, 6.11 (t, *meta*, J(H) 7.0)
				6.17 (t, *para*, J(H) 7.0)
				6.94 (m, *ortho*, obscured)
5: R = CH$_3$; R′ = CH$_2$SiMe$_3$	0.15 (s)	1.87 (dt, J_{app} 6, J_{gem} 13)	7.18 (m, *meta* / *para*)	Ir–CH_3, 1.51 (t, J(P) 6)
	0.54 (s)	2.05 (dt, J_{app} 4)	7.63 (m, *ortho*)	Ir–CH_2Si(CH$_3$)$_3$, 0.51 (t, J(P) 8)
			7.89 (m, *ortho*)	Ir–CH$_2$Si(CH_3)$_3$, 0.0 (s)
6: R = R′ = C$_6$H$_5$	0.23 (s)	1.85 (t, J_{app} 5.0)	6.92 (m, *meta* / *para*)	Ir–(C$_6$$H_5$)$_2$, 6.71 (t, *meta*, J(H) 8.0)
			7.31 (m, *ortho*)	6.79 (t, *para* J(H) 8.0)
				7.31 (m, *ortho*, obscured)
7: R = C$_6$H$_5$; R′ = CH$_2$CMe$_3$	0.40 (s)	1.74 (dt, J_{app} 5.1, J_{gem} 13.5)	7.01 (m, *meta* / *para*)	Ir–CH_2C(CH$_3$)$_3$, 2.24 (t, J(P) 8)
	0.62 (s)	2.07 (dt, J_{app} 5.1)	7.22 (m, *ortho*)	Ir–CH$_2$C(CH)$_3$)$_3$, 0.88 (s)
			7.45 (m, *ortho*)	Ir–C$_6$H$_5$, 6.81 (br, *meta*)
				6.87 (t, *para*, J(P) 8)
				7.01 (m, *ortho*, obscured)

8: R = CH_2Ph; R′ = CH_3	−0.02 (s)	1.68 (dt, J_{app} 4.9, J_{gem} 12.9)	7.23 (m, *meta/para*)	Ir–CH_3, 1.50 (t, J(P) 5.5)
	0.20 (s)	1.79 (dt, J_{app} 4.9)	7.55 (m, *ortho*)	Ir–C$H_2C_6H_5$, 2.71 (t, J(P) 6.9)
			7.80 (m, *ortho*)	Ir–$CH_2C_6$$H_5$, 7.23 (m, obscured)
9: R = R′ = CH_2Ph	0.24 (s)	1.72 (t, J_{app} 5)	7.02 (m, *meta/para*)	Ir–C$H_2C_6H_5$, 3.38 (t, J(P) 6)
			7.53 (m, *ortho*)	Ir–$CH_2C_6$$H_5$, 6.76 (t, *meta*, J(H) 8)
				6.92 (t, *para*, J(H) 8)
				6.97 (d, *ortho*, J(H) 8)
10: R = CH_2Ph; R′ = CH_2SiMe_3	0.42 (s)	1.98 (dt, J_{app} 4.7, J_{gem} 13.0)	7.21 (m, *meta/para*)	Ir–C$H_2C_6H_5$, 3.40 (t, J(P) 5.6)
	0.45 (s)	1.84 (dt, J_{app} 4.7)	7.63 (m, *ortho*)	Ir–$CH_2C_6$$H_5$, 6.88 (t, *meta*, J(H) 7.5)
			7.77 (m, *ortho*)	7.07 (m, *para*, obscured)
				7.11 (m, *ortho*, obscured)
				Ir–CH_2Si(CH_3)$_3$, 0.80 (t, J(P) 7.5)
				Ir–CH_2Si(CH_3)$_3$, −0.05 (s)
11: R = CH_2Ph; R′ = C_6H_5	0.23 (s)	1.55 (dt, J_{app} 5.0, J_{gem} 13.0)	6.95 (m, *meta/para*)	Ir–C$H_2C_6H_5$, 3.42 (*t*, J(P) 6.6)
	0.27 (s)	1.76 (dt, J_{app} 5.0)	7.31 (m, *ortho*)	Ir–$CH_2C_6$$H_5$, 6.95 (m, obscured)
			7.51 (m, *ortho*)	Ir-$C_6$$H_5$, 6.95 (m, obscured)

---

[a] All spectra recorded at 25 °C in C_6D_6 at 300 MHz or 400 MHz and referenced to C_6H_5*H* at 7.15 ppm; all J values are given in Hertz. $J_{app} = \frac{1}{2}|^2J(PH)) + ^4J(PH)|$ and is half the distance between the two outer lines of the virtual triplet.

Table 5

$^{13}C\{^1H\}$ NMR spectral data for the complexes $Ir(R)R'[N(SiMe_2CH_2PPh_2)_2]$ [a]

Complex [b]	$Si(CH_3)_2$	PCH_2Si	$P(C_6H_5)_2$	Other
$Ir\{PNP\}(CH_3)_2$	5.09 (s)	24.90 (t, J_{app} 6.7)	$C1$, 134.42 (t, J_{app} 48.7) $C2$,$C6$, 134.16 (t, J_{app} 5.8) $C3$,$C5$, 128.06 (obscured) $C4$, 129.69 (s)	$Ir-CH_3$, −27.71 (t, J(P) 4.7)
$Ir\{PNP\}(Ch_3)[CH_2C(CH_3)_3]$	4.74 (s) 6.36 (t, J_{app} 4.4)	24.98 (t, J_{app} 6.4)	$C1$, 138.45 (t, J_{app} 25.2) 131.70 (t, J_{app} 20.2) $C2$,$C6$, 135.47 (t, J_{app} 6.1) 132.91 (t, J_{app} 5.0) $C3$,$C5$, 128.15 (obscured) C_4, 129.57 (s) 129.78 (s)	Ir CH_3, −28.45 (t, J(P) 6.8) $Ir-CH_2C(CH_3)_3$, 16.34 (t, J(P) 3.1) $Ir-CH_2C(CH_3)_3$, 34.95 (s) Ir $CH_2C(CH_3)_3$, 31.94(s)
$Ir\{PNP\}(CH_3)(C_6H_5)$	5.28 (s) 5.36 (s)	23.10 (t, J_{app} 7.1)	$C1$, $C2$,$C6$, 134.43 (t, J_{app} 5.3) 133.91 (t, J_{app} 5.6) $C3$,$C5$, 127.95 (obscured) $C4$, 129.69 (s) 129.87 (s)	$Ir-CH_3$, −22.06 (t, J(P) 4.6) $Ir-C_6H_5$, $C1$, 127.15 (t, J(P) 6.8) $C2$,$C6$, 137.35 (t, J(P) 3.3) $C3$,$C5$, 126.25 (s) $C4$, 120.84 (s)
$Ir\{PNP\}(CH_3)[CH_2Si(CH_3)_3]$	4.81 (s) 6.16 (t, J_{app} 4.1)	24.76 (t, J_{app} 6.4)	$C1$, 137.38 (t, J_{app} 24.7) 131.71 (t, J_{app} 18.4) $C2$,$C6$, 135.53 (t, J_{app} 6.1) 133.08 (t, J_{app} 4.8) $C3$,$C5$, 127.70 (s) 128.34 (s) $C4$, 129.70 (s) 129.94 (s)	Ir CH_3, −27.93 (t, J(P) 6.1) $Ir-CH_2Si(CH_3)_3$, −14.37 (s) $Ir-CH_2Si(CH_3)_3$ 2.24 (s)
$Ir\{PNP\}(C_6H_5)_2$	5.01 (s)	22.84 (t, J_{app} 8.1)	$C1$, 133.59 (t, J_{app} 23.9) $C2$,$C6$, 134.41 (t, J_{app} 5.6) $C3$,$C5$, 127.60 (obscured) $C4$, 129.77 (s)	$Ir-C_6H_5$, $C1$, 125.64 (t, J(P) 7.0) $C2$,$C6$, 138.80 (t, J(P) 3.5) $C3$,$C5$, 126.13 (s) $C4$, 121.39 (s)
$Ir\{PNP\}(C_5H_5)[CH_2C(CH_3)_3]$	6.03 (s)	23.87 (t, J_{app} 7.1)	$C1$, 129.95 (t, J_{app} 21.1)	$Ir-C_6H_5$, $C1$

	6.60 (t, J_{app} 3.6)		137.48 (t, J_{app} 25.6)	C2,C6
			C2,C6, 134.09 (t, J_{app} 6.0)	C3,C5, 125.26 (s)
			133.42 (t, J_{app} 4.9)	C4, 121.61 (s)
			C3,C5, 127.93 (obscured)	Ir–$CH_2C(CH_3)_3$, 20.45(s)
			C4, 129.47 (s)	Ir–$CH_2C(CH_3)_3$, 35.64 (s)
			129.77(s)	Ir–$CH_2C(CH_3)_3$, 41.49(s)
Ir{PNP}($CH_2C_6H_5$)(CH_3)	4.67 (s)	24.29 (t, J_{app} 6.7)	C1, 132.82 (t, J_{app} 20.7)	Ir–$CH_2C_6H_5$, 2.60 (s)
	5.59 (t, J_{app} 3.9)		136.77 (t, J_{app} 24.5)	Ir–$CH_2C_6H_5$, C1
			C2,C6, 133.06 (t, J_{app} 4.8)	C2,C6, 133.46 (t, J(P) 4.9)
			135.51 (t, J_{app} 6.2)	C3,C5, 127.64 (s)
			C3,C5, 128.2 (obscured)	C4, 124.25 (s)
			C4,	Ir–CH_3, 31.60 (t, J(P) 5.3)
Ir{PNP}($CH_2C_6H_5$)[$CH_2Si(CH_3)_3$]	6.03 (s)	22.14 (t, J_{app} 7.3)	C1	Ir–$CH_2C_6H_5$, −1.46 (t, J(P) 3.1)
	4.82 (s)			Ir–$CH_2C_6H_5$, C1, 151.40 (s)
			C2,C6, 133.65 (t, J_{app} 5.5)	C2,C6
			134.25 (t, J_{app} 5.6)	C3,C5
			C3,C5, 128.60 (obscured)	C4
			C4	Ir–$CH_2Si(CH_3)_3$, −24.22 (t, J(P) 4.1)
				Ir–$CH_2Si(CH_3)_3$, 2.57 (s)
Ir{PNP}($CH_2C_6H_5$)$_2$	4.74 (s)	21.88 (t, J_{app} 7.7)	C_1, 134.12 (t, J_{app} 22.0)	Ir–$CH_2C_6H_5$, −4.22 (t, J(P) 3.6)
			C2,C6, 133.59 (t, J_{app} 5.4)	Ir–$CH_2C_6H_5$, C1, 151.86 (s)
			C3,C5, 128.10 (obscured)	C2,C6,
			C4,	C3,C5,
				C4, 123.78 (s)
Ir{PNP}($CH_2C_6H_5$)(C_6H_5)	5.53 (s)	23.17 (t, J_{app} 7.7)	C1, 131.76 (t, J_{app} 22.6)	Ir–$CH_2C_6H_5$, 4.13 (s)
			135.57 (t, J_{app} 24.4)	Ir–$CH_2C_6H_5$, C1, 151.77 (s)
			C2,C6, 133.75 (t, J_{app} 5.2)	C2,C6
			134.45 (t, J_{app} 5.8)	C3,C5
			C3,C5, 127.91 (obscured)	C4
				Ir–C_6H_5, C1, 120.76 (t, J(P) 7.7)
			C4	C2,C6
				C3,C5
				C4

---

[a] All spectra recorded at 25 °C in C_6D_6 at 75.43 MHz and referenced to C_5CD_6 at 128.00 ppm; all J values are given in Hertz. $J_{app} = \frac{1}{2}|{}^2J(PH)+{}^4J(PH)|$ and is half the distance between the outer lines of the virtual triplet. [b] {PNP} = [$N(SiMe_2CH_2PPh_2)_2$].

benzyl bromide (**1b**) and phenyl iodide (**1c**) complexes also show the expected enhancement in the Ir–CH_2Ph and the ortho protons of the iridium-phenyl group when the appropriate, respective methylene resonances are irradiated. However, the analogous NOE results are not observed upon irradiation of the ligand methylene protons of the bis(hydrocarbyl) complexes. For example, the NOEDIFF spectrum for compound **3** does not show any enhancement for the Ir–CH_3 nor for the Ir–CH_2CMe$_3$ on irradiation of either set of methylene protons on the backbone of the ancillary ligand. The diphenyl (**6**) and the dibenzyl (**9**) complexes also show no enhancement of the appropriate resonances of the hydrocarbyl group when the ligand methylene protons are pulsed in a NOEDIFF experiment. Indeed, all of the complexes **2**–**11** give analogous results and are therefore considered to have a different geometry than the hydrocarbyl halide complexes **1**. Given that both sets of complexes are five-coordinate with the latter complexes having a square-pyramidal structure, the inescapable conclusion is that the bis(hydrocarbyl) derivatives are trigonal bipyramidal. This is consistent with the accepted origin of the NOE [26] as a through-space transfer of magnetization that varies a $1/r^6$; thus, in the square-pyramidal geometry, the apical hydrocarbyl ligand is closer to the methylene protons of the ligand backbone than in the trigonal bipyramidal geometry where the hydrocarbyl groups are in the equatorial plane. Additional evidence supporting this conclusion are the X-ray crystal structures of the methyl neopentyl complexes **3** [24] and the dibenzyl derivative **9**.

X-ray crystallographic information

Shown in Fig. 1 is the molecular structure of the dibenzyl derivative $Ir(CH_2Ph)_2[N(SiMe_2CH_2PPh_2)_2]$ (**9**), as determined by X-ray crystallographic analysis. The molecule is best described as having a trigonal-bipyramidal configuration, very similar to that observed for the methylneopentyl complex **3**, the structure of which was reported in a previous communication [24]. In particular, the iridium–carbon bond lengths of 2.113(3) Å (Ir–C38) and 2.102(3) Å (Ir–C31) are significantly different as was observed for the methylneopentyl complex **3**: 2.131(9) and 2.089(9) Å. The angle between the axial phosphorus donors of **9** is 170.25(5)° as compared to 168.45(9)° found in **3**. The largest distortion from ideal trigonal-bipyramidal geometry for both complexes is the angle subtended by the two alkyl ligands. Considerably less than the 120° expected, the angle measures only 77.6(1)° and 76.0(4)° for the dibenzyl and methylneopentyl compounds, respectively. Interestingly, the isoelectronic, five-coordinate hydridophenyl complex, $Ir(C_6H_5)H(PPr^i_3)_2Cl$ [27], also shows such a small angle of 77.9° in the equatorial plane between the phenyl and hydride substituents. The closing down of this equatorial angle has been predicted [28] by a theoretical calculation for d^6 five-coordinate complexes. On the basis of extended Hückel calculations, it was concluded that a trigonal bipyramidal geometry would actually by stabilized by an angular deformation in the equatorial plane in the form of a decrease in one of the angles from 120 to 90°. Moreover, it was pointed out that strong σ-donor ligands subtending this angle would further stabilize the trigonal-bipyramidal form by removing a degeneracy and preventing destabilization by a first order Jahn–Teller effect. A rather different set of ligands around iridium, as found in $Ir(O_2CCF_3)_2NO(PPh_3)_2$ [29], also results in a trigonal bipyramidal geometry with a similar angle distortion in the equatorial plane; the angle O–Ir–O is 75.0(6)°. Taken together, these results tend to

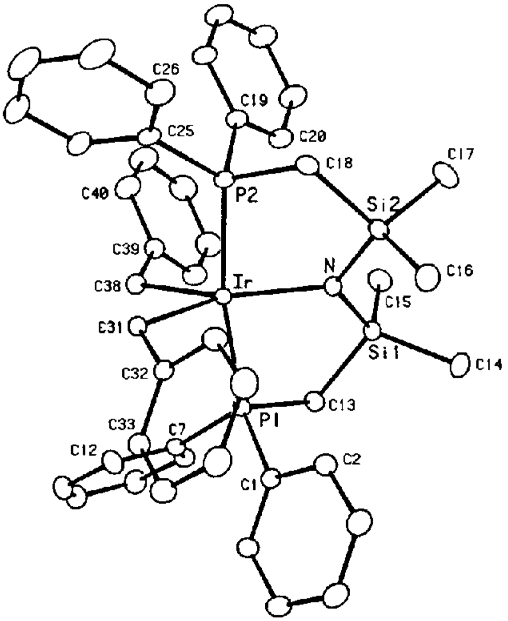

Fig. 1. Perspective view of the molecule showing the atom numbering scheme. The phenyl rings are numbered sequentially around the ring. Atoms are represented by thermal ellipsoids at the 20% probability level. The H atoms have been omitted for clarity.

support the importance of the σ-donor ability of the equatorial ligands in stabilizing the trigonal bipyramidal form and distorting the equatorial angle.

Another facet of the theoretical study [28] mentioned above was the prediction that single-faced π-donors should also help stabilize the trigonal bipyramidal form over the square-pyramidal geometry; for example, an amide, $^-NR_2$, is a single-faced donor while a chloride can be considered as a double-faced π-donor. This was reasoned by considering that the most favorable overlap between the single, filled *p* orbital on the amide and an empty suitable orbital on the metal, would occur in the trigonal bipyramidal geometry in the equatorial plane. Our ancillary ligand is precisely set up for this since the filled *p* orbital on the amides lies coplanar with the equatorial ligands. However, examination of the Ir–N bond lengths for a variety of complexes does not provide conclusive evidence for such an overlap. While the Ir–N bond length in **9** is 2.113(3) Å and is identical to that found [24] in the methylneopentyl complex **3** of 2.109(7) Å, these are approx. 0.03 Å longer than that found for two other iridium amide complexes: the five-coordinate, square pyramidal $Ir(CH_3)I[N(SiMe_2CH_2PPr^i_2)_2]$ has an Ir–N length of 2.079(5) Å [11], and the Ir–N length in the square planar methylidene complex $Ir(=CH_2)[N(SiMe_2CH_2PPh_2)_2]$ is 2.080 (9) Å [23]. The alternative argument, that all of these complexes are stabilized by some *π-p-d* contribution resulting in short Ir–N bonds, is of course tenable. Iridium amides are such rare species [30] that arguments requiring a reasonable sample of examples, such as a series of Ir–N bondlengths, are difficult to substantiate.

Conclusion

The straightforward synthesis and characterization of the complexes as described above has provided a facile route for the production of bis(hydrocarbyl)iridium(III) complexes. These five-coordinate complexes have trigonal bipyramidal structures both in solution, as determined by NOEDIFF experiments, and in the solid state, as determined by single crystal X-ray diffraction. Although thermally stable, these complexes have been found to undergo some interesting photochemical reactions. A previous report [23] from our laboratory described the first example of a square planar methylideneiridium complex, produced upon the irradiation of $Ir(CH_3)CH_2CMe_3[N(SiMe_2CH_2PPh_2)_2]$. The photochemistry of a number of these bis(hydrocarbyl) compounds as well as speculation on the mechanism of the alkylidene formation will be the subject of a future publication.

Acknowledgements

Financial support was provided by NSERC of Canada. We are grateful to Johnson–Matthey for the generous loan of $IrCl_3$.

References

1 G. Leigh and R.L. Richards, in G. Wilkinson, R.D. Gillard, J.A. McCleverty (Eds.), Comprehensive Organometallic Chemistry, Pergamon Press, Oxford, 1987, Volume 5, Chapter 36, p. 541.

2 J.P. Collman, L.S. Hegedus, J.R. Norton, R.G. Finke, Principles and Applications of Organotransition Metal Chemistry, University Science Books, Mill Valley, Chem. Abstr., (1987) pp. 4–6.

3 J.D. Atwood, Coord. Chem. Rev., 83 (1988) 93.

4 R.H. Crabtree, Chem. Rev., 85 (1985) 245.

5 (a) L. Vaska and J.W. DiLuzio, J. Am. Chem. Soc., 84 (1962) 679; (b) J. Chatt and A.E. Underhill, J. Chem. Soc., (1963) 2088; (c) R.F. Heck, J. Am. Chem. Soc., 86 (1964) 2796; (d) P.B. Chock and J. Halpern, J. Am. Chem. Soc., 88 (1966) 3511; (e) J. Chatt and B.L. Shaw, J. Chem. Soc. A, (1966) 1836; (f) J. Chatt, N.P. Johnson and B.L. Shaw, ibid., (1967) 604; (g) B.L. Shaw and A.C. Smithies, ibid., (1967) 1047; (h) N.A. Bailey, C.J. Jones, B.L. Shaw and E. Singleton, J. Chem. Soc., Chem. Commun., (1967) 1051; (i) B.L. Shaw and E. Singleton, J. Chem. Soc. A, (1967) 1683; (j) A.J. Deeming and B.L. Shaw, ibid., (1969) 1128; (k) M. Kubota and D.M. Blake, J. Am. Chem. Soc., 93 (1971) 1368; (l) M. Kubota, D.M. Blake and S.A. Smith, Inorg. Chem., 10 (1971) 1430; (m) M.A. Bennett and R. Charles, J. Am. Chem. Soc., 94 (1972) 666; (n) B.E. Mann, B.L. Shaw and R.E. Stainbank, J. Chem. Soc., Chem. Commun., (1972) 151; (o) M.A. Bennett, R. Charles and T.R.B. Mitchell, J. Am. Chem. Soc., 100 (1978) 2737; (p) M.A. Bennett and J.C. Jeffery, Inorg. Chem., 19 (1980) 3763; (q) T.H. Tulip and D.L. Thorn, J. Am. Chem. Soc., 103 (1981) 2448; (r) D.L. Thorn and T.H. Tulip, ibid., 103 (1981) 5986; (s) N.L. Jones and J.A. Ibers, Organometallics, 2 (1983) 490; (t) K.A. Bernard and J.D. Atwood, ibid., 6 (1987) 1133; (u) M. Kubota, T.M. McCleskey, R.K. Hayashi and C.G. Webb, J. Am. Chem. Soc., 109 (1987), 7569.

6 (a) K. Isobe, P.M. Bailey and P.M. Maitlis, J. Chem. Soc., Chem. Commun., (1981) 808; (b) A.H. Janowicz and R.G. Bergman, J. Am. Chem. Soc., 104 (1982) 352; (c) J.K. Hoyano and W.A.G. Graham, ibid., 104 (1982) 3723; (d) A.H. Janowicz and R.G. Bergman, ibid., 105 (1983) 3929; (e) J.K. Hoyano, A.D. McMaster and W.A.G. Graham, ibid., 105 (1983) 7190; (f) M. Gomez, D.J. Robinson, and P.M. Maitlis, J. Chem. Soc., Chem. Commun., (1983) 825. (g) A.J. Rest, I. Whitwell, W.A.G. Graham, J.K. Hoyano and A.D. McMaster, ibid., (1984) 624; (h) M.J. Wax, J.M. Stryker, J.M. Buchanan, C.A. Kovac and R.G. Bergman, J. Am. Chem. Soc., 106 (1984) 1121; (i) A.H. Janowicz, R.A. Periana, J.M. Buchanan, C.A. Kovac, J.M. Stryker, M.J. Wax, and R.G. Bergman, Pure Appl. Chem., 56 (1984) 13; (j) M. Buchanan, J.M. Stryker and R.G. Bergman, J. Am. Chem. Soc., 108 (1986) 1537; (k) S.P. Nolan, C.D. Hoff, P.O. Stoutland, L.J. Newman, J.M. Buchanan, R.G. Bergman, G.K. Yang and K.S. Peters, ibid., 109 (1987) 3143; (l) A.J. Rest, I. Whitwell, W.A.G. Graham, J.K. Hoyano and A.D. McMaster, J. Chem. Soc., Dalton Trans., (1987) 1181.

7 (a) M.D. Rausch and G.A. Moser, Inorg. Chem., 13 (1974) 11; (b) L. Dahlenburg, F. Mirzaei, A. Yardimcioglu and R. Nast, Z. Naturforsch, B, 37 (1982) 310; (c) L. Dahlenburg and R. Nast, J. Organomet. Chem., 110 (1976) 395; (d) L. Dahlenburg and F. Mirzaei, ibid., 251 (1983) 11. (e) L. Dahlenburg, ibid., 251 (1983) 347; (f) E. Arpac and L. Dahlenburg, ibid., 251 (1983) 361; (g) L. Dahlenburg and C. Prengel, Organmetallics, 3 (1984) 934. (h) W.M. Rees, M.R. Churchill, Y.J. Li and J.D. Atwood, ibid., 4 (1985) 1162; (i) L. Dahlenburg, F. Mirzaei and B. Pietsch, Inorg. Chim. Acta, 97 (1985) L5; (j) B.J. Rappoli, M.R. Churchill, T.S. Janik, W.M. Rees and J.D. Atwood, J. Am. Chem. Soc., 109 (1987) 5145; (k) A.A. Del Paggio, R.A. Andersen and E.L. Muetterties, Organometallics, 6 (1987) 1260.

8 (a) J.R. Shapley and J.A. Osborn, J. Am. Chem. Soc., 92 (1970) 6976; (b) G. Yagupsky and C.K. Brown, J. Chem. Soc. A, (1970) 1392; (c) M.R. Churchill and S.A. Bezman, Inorg. Chem., 12 (1973) 531; (d) L. Dahlenburg and F. Mirzaei, J. Organomet. Chem., 251 (1983) 123; (e) L. Dahlenburg and F. Mirzaei, Inorg. Chim. Acta, 97 (1985) L1; (f) L. Dahlenburg and A. Yardimcioglu, J. Organomet. Chem., 299 (1986) 149; (g) W.M. Rees, M.R. Churchill, J.C. Fettinger and J.D. Atwood, ibid., 319 (1987) 411.

9 M.D. Fryzuk, P.A. MacNeil and S.J. Rettig, J. Organomet. Chem., 332 (1987) 345.

10 M.D. Fryzuk, D.J. Berg and T.S. Haddad, unpublished results.

11 M.D. Fryzuk, P.A. MacNeil, and S.J. Rettig, Organometallics, 5 (1986) 2469.

12 R.R. Schrock and J.D. Fellmann, J. Am. Chem. Soc., 100 (1978) 3359.

13 M. Schlosser and V. Ladenberger, J. Organomet. Chem., 8 (1967) 193.

14 M.R. Collier, M.F. Lappert and R. Pearce, J. Chem. Soc., Dalton Trans., (1973) 445.

15 G.G. Eberhardt and W.A. Butte, J. Org. Chem., 29 (1964) 2928.

16 An alternate synthetic method for compounds where $R' = CH_2C_6H_5$ involved using $KCH_2C_6H_5$ dissolved in THF. M. Schlosser and J. Hartmann, Angew. Chem., Engl. Ed., 12 (1973) 508.

17 The diffractometer programs are those supplied by Enraf–Nonius for operating the CAD4F diffractometer with some local modifications and additions.

18 International Tables for X-ray Crystallography, Kynoch Press, Birmingham, England, 1969, Vol. I.

19 N. Walker and D. Stuart, Acta. Crystallogr. A., 39 (1983) 158.

20 The computer programs used in this analysis include the Enraf–Nonius Structure Determination Package by B.A. Frenz (Computing in Crystallography, Delft University Press, Delft, Holland, 1978, p. 64–71) and several locally written or modified programs.

21 International Tables for X-ray Crystallography, Kynoch Press, Birmingham, England, 1974, Vol. IV, Table 2.2B.

22 Ref. 21, Table 2.3.1.

23 M.D. Fryzuk, P.A. MacNeil, and S.J. Rettig, J. Am. Chem. Soc., 107 (1985) 6708.

24 M.D. Fryzuk, P.A. MacNeil, and R.G. Ball, J. Am. Chem. Soc. 108 (1986) 6414.

25 M.D. Fryzuk, P.A. MacNeil, N.T. McManus, Organometallics, 6 (1987) 882.

26 J.K. Saunders and J.W. Easton, in F.C. Nachod, J.J. Zuckerman and E.W. Randall, (Eds.), The Determination of Organic Structures by Physical Methods, Academic Press, New York, 1976, Vol. 6, p. 271.

27 H. Werner, A. Höhn and M. Dziallas, Angew. Chem., 98 (1986) 1112.

28 D.L. Thorn and R. Hoffmann, Nouv. J. Chim., 3 (1979) 39.

29 A. Dobson, D.S. Moore, S.D. Robinson, A.M.R. Galas, and M.B. Hursthouse, J. Chem. Soc. Dalton Trans., (1985) 611.

30 M.D. Fryzuk and C.D. Montgomery, Coord. Chem. Rev., in press.